

Received 18 October 2023, accepted 5 November 2023, date of publication 8 November 2023, date of current version 15 November 2023.

Digital Object Identifier 10.1109/ACCESS.2023.3331431

RESEARCH ARTICLE

Characterization of Resistance and Inductance of PIN Diode at mmWave Frequency Using 7-Layer Deep Neural Network

LIHOUR NOV^{1,2}, (Student Member, IEEE), THORN CHREK^{2,3},
AND JAE-YOUNG CHUNG^{2,3}, (Senior Member, IEEE)

¹Department of Integrated IT Engineering, Seoul National University of Science and Technology, Seoul 01811, South Korea

²Research Center for Electrical and Technology, Seoul National University of Science and Technology, Seoul 01811, South Korea

³Department of Electrical and Information Engineering, Seoul National University of Science and Technology, Seoul 01811, South Korea

Corresponding author: Jae-Young Chung (jychung@seoultech.ac.kr)


This work was supported by the National Research Foundation of Korea (NRF) Grant funded by the Korea Government (MSIT) under Grant 2021R1A2C1095134.

ABSTRACT This paper presents a novel technique for extracting the resistance (R) and inductance (L) of an ultra-low capacitance PIN diode, a critical component in developing 5G mmWave reconfigurable circuits and antennas. In the proposed method, a PIN diode is mounted on a microstrip transmission line and biased by a DC biasing network and its S-parameters are measured. The measured S-parameters are calibrated by the thru-reflect-line calibration to reduce undesirable effects from the measurement fixture. Subsequently, the post-calibration transmission coefficient (S_{21}) is fed into a deep neural network (DNN) which has been trained with simulated S_{21} data obtained from a full-wave 3D electromagnetic simulation software. The output of the DNN provides frequency dependent R and L values at the frequency range from 27 GHz to 30 GHz. The results agree well the presumption that R decreases with the increase in bias current and frequency, while L increases as the frequency increases. This result was obtained with a MA4AGP907 p-i-n diode biased with three different forward currents i.e. 1 mA, 5 mA, and 7 mA.

INDEX TERMS Deep neural network (DNN), p-i-n diode, equivalent circuit, mmWave, TRL calibration.

I. INTRODUCTION

Reconfigurable antennas have played a significant role in recent wireless communication technologies due to their flexibility in operations, especially in the context of the fifth generation (5G) [1], [2], [3]. These antennas enables a compact design footprint of the antenna system due to their multipurpose operational capabilities as the antenna geometry can be adjusted dynamically. The reconfigurable properties may include a frequency, pattern, polarization reconfigurability, or a combination of these properties [4], [5], [6]. For instance, a pattern-reconfigurable antenna can provide multiple switchable beams that significantly enhances the channel capacity, efficiency, and coverage of the transmission system in urban vehicle communication [1].

The associate editor coordinating the review of this manuscript and approving it for publication was Wanchen Yang .

In practice, reconfigurable antennas can be realized by employing various mechanisms, including changes in material, optical, mechanical, and electrical characteristics [4]. Electrical reconfigurability mechanism has become a promising solution for the development of modern reconfigurable antennas due to its simplicity and compact design. This mechanism utilizes radio frequency micro-electromechanical-systems (RF MEMS) [7], varactor diodes [8], and p-i-n diodes [1], [9], [10], to modify the properties of the antenna electrically. Among these components, a reconfigurable antenna using p-i-n diodes is widely developed due to its fast-switching speed, low cost, precision control, and easy integration capability [1], [9].

The p-i-n diode, which is a current-controlled resistor at RF/Microwave frequency, is typically integrated into the design of reconfigurable antenna to effectively modify the electrical characteristics [2]. Fig. 1 depicts a sample image

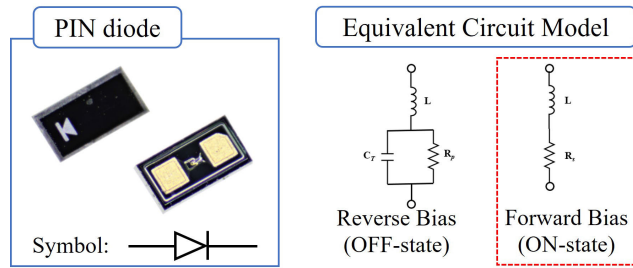


FIGURE 1. p-i-n diode sample and its equivalent circuit model [11], where R_s is the series resistance under forward bias, and R_p is the resistance connected in parallel with the total capacitance C_T in the reverse bias.

of a p-i-n diode and the representative equivalent circuit in its forward and reverse bias state, respectively [11]. Electrical characteristics of a p-i-n diode, e.g., R-L parameters in forward bias, are crucial for designing and optimizing the performance of reconfigurable antenna. For example, a small change in the forward state resistance of the p-i-n diode shifts the resonant frequency of the antenna [12], [13]. Therefore, accurate knowledge of the electrical parameters of the diode must be obtained prior to designing and optimizing the reconfigurable antenna. This parasitic component can cause severe degradation in the overall system performance due to inaccurate and unpredictable antenna characteristics [14]. For this reason, a suitable method that can accurately predict the parasitic elements of the equivalent circuit for the p-i-n diode model is always in demand.

Many researchers utilize specifications supplied by the manufacturer to reflect p-i-n diode behavior, which is limited to specific bias conditions or low frequencies [1], [2], [5]. To overcome the above issue, researchers have estimated the electrical parameters of a diode with measured S-parameter data in combination with an in-house extraction method e.g., curve-fitting or analytical ABCD matrix [15], [16], [17]. For instance, the curve-fitting method extracts the R-L parameters of the diode by fitting its data to a equivalent circuit obtained from a T-model or π -model. However, it only provides a rough approximation of the results at a single frequency point, and the accuracy is heavily rely on that representation mathematical model. Additionally, the fitting parameters are often correlated, making it challenging to extract individual electrical parameters of the diode. It is also sensitive to noise in the measured data since small fluctuations can lead to severe errors in the extracted results, particularly at high frequencies when the signal-to-noise ratio is often low. An alternative method involving machine learning (ML) to analyze the diode characteristics also exists, but it only addresses overall system performance analysis without directly extracting the electrical parameters of the diode [18].

In this paper, we present a novel technique to extract the parasitic properties of the MA4AGP907 p-i-n diode in its forward bias state, specifically the R-L electrical parameters

since it is commonly used for developing a 5G high band reconfigurable antenna [1], [10]. We designed a microstrip transmission line (tx-line), incorporating a DC biasing network and corresponding thru-reflect-line (TRL) calibration tx-line standards [19]. The calibration enables accurate extraction of the responses of the p-i-n diode while mitigating unwanted effects stemming from the measurement fixture. An optimal 7-hidden layer deep neural network (DNN) model is proposed to extract the electrical parameters of the diode, which has been trained with simulated data obtained from a full-wave 3D electromagnetic simulation software (HFSS). From the measured calibrated data of the diode, we have successfully obtained its R-L electrical parameters over a frequency range spanning from 27 GHz to 30 GHz at various DC biasing currents, including 1 mA, 5 mA, and 7 mA.

This paper is organized as follows. Section II provides an overview of the procedure for extracting the R-L parameters of the p-i-n diode, starting from the design stage of the proposed measurement fixture and culminating in the final prediction stage using our in-house developed DNN model. We also describe the design of the measurement fixture and its corresponding TRL calibration, and the development of our proposed 7-hidden layer DNN model. Section III presents the measurement setup and data collection process for the measured p-i-n diode model, based on our configuration of the applied DC forward biasing conditions. Section IV describes the measurement process and presents the calibrated results, followed by extracting the R-L electrical parameters of the p-i-n diode. Finally, we summarize the primary contributions of this work and provide a conclusion to our research in Section V.

II. PROPOSED CHARACTERIZATION METHOD AND IMPLEMENTATION

The flow chart in Fig. 2 illustrates the entire parameter extraction process, encompassing two primary steps: the design of the measurement fixture and the development of the DNN model for extracting the R-L electrical parameters. Initially, we must identify a suitable measurement fixture that is capable of integrating a DC biasing network to activate the functionality of the diode. It is important to emphasize that solely the S_{21} of the diode will be utilized to retrieve the R-L electrical parameters. This necessitates an additional design and implementation phase for the TRL calibration. Lastly, the calibrated measurement responses are fed into the optimally trained DNN model to estimate the electrical parameters of the p-i-n diode. The details of the above-mentioned steps are provided in the following subsection.

A. PROPOSED DESIGN OF MEASUREMENT FIXTURE

In our method, we employ a microstrip line based measurement fixture. It contains a DC biasing circuit to control the PIN diode providing different biasing points. It is worth emphasizing that this research aims to attain a more accurate

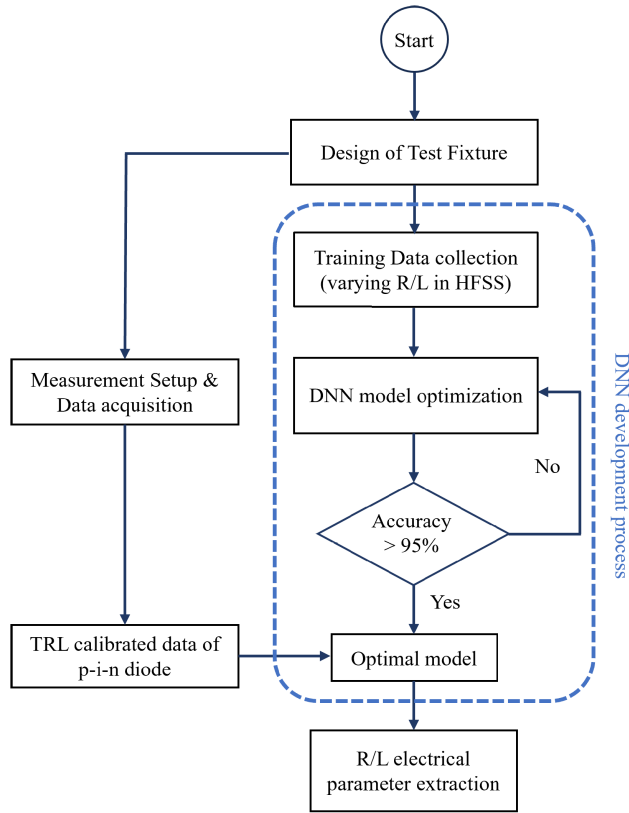


FIGURE 2. Flow chart of the proposed method.

estimation of the electrical parameters to the p-i-n diode, particularly in its forward bias state. We try to encompass every conceivable factors that might significantly influence the overall performance of the characterization results. So, we deliberately incorporated the DC bias circuit into the design of the fixture in which the microstrip configuration is the most promising structure for this purpose. The fixture incorporated a single-pole-single-throw (SPST) DC biasing mechanism which encompasses a series DC blocking capacitor and a shunt RF choke. Fig. 3 provides a visual representation of the comprehensive design of the proposed measurement fixture.

The microstrip was designed to operate at the frequency of 28 GHz with a 50 Ω impedance standard, utilizing an RT/Duriod 5880 substrate (Dk = 2.20, Df = 0.0009) with a thickness of 0.508 mm. We designed a quarter wave transformer (QWT) for impedance transition to minimize the impedance mismatches between the microstrip trace line and the 2.92 mm connector (DC – 40 GHz). The overall design integrates an interdigital capacitor (IDC) [20], and a radial stub [21] to mitigate parasitic effects arising from the non-ideal behavior of the low-frequency lumped components in the DC biasing network. Design parameters essential for the proposed measurement fixture (see Fig. 1) are presented in Table 1. From the DUT fixture, we also design the three corresponding Thru-, Reflect, and Line tx-line standards for TRL calibration.

TABLE 1. Design parameters of the proposed measurement fixture.

Design parameter	Description	Value (mm)
Mic_tl	Microstrip trace line width	0.77
IDC_g	Gap of the IDC	0.10
IDC_fl	Finger length of the IDC	2.30
IDC_fw	Finger width of the IDC	0.19
Rad_lw	Line width of the radial stub	0.20
Rad_r	Radius of the radial stub	1.67
Dis_rad	Distance between the two radial stubs	1.81
Con_t	Thickness of the conductor	0.018
Sub_t	Thickness of the substrate	0.508

B. DEVELOPMENT OF THE DNN MODEL

Another significant component of the proposed method involves utilizing a DNN-based extraction approach, particularly a supervised feed-forward network, to characterize the R-L electrical parameter of the p-i-n diode. This AI-inspired algorithm allows the computer to learn from known training input data and makes predictions on other unknown data based on the optimally trained model [22], [23], [24]. The model consists of three main layers such as the input layer, the hidden layer, and the output layer. The calibrated S_{21} complex data is used as the input, while the R/L electrical parameter is used as the output. The hidden layers encompass multiple perceptrons, which are processing nodes computed from a weighted sum model by assigning random weights for each corresponding input and introducing a bias to generate individual outputs. The outputs of each perceptron in the first hidden layer are then forwarded as inputs to the second hidden layer with its corresponding bias. This process continues until the final hidden layer is reached, and a suitable activation function, e.g., scaled exponential linear unit (SELU), is employed to retrieve the output. The mean squared error (MSE) is utilized as a cost function to estimate the error between the actual and the predicted result. The cost function is then minimized by using the Adam optimizer, which employs the backpropagation algorithm to provide suitable updated values for the weights and biases [24].

Fig. 4(a) illustrates the single-frequency DNN model for extracting the R-L electrical parameter of the p-i-n diode from the S_{21} complex data. We introduced a 7-hidden layer DNN model featuring a rhombus-shaped hidden layer structure, wherein the number of the perceptrons is doubled at layer transitions from the first to the fourth layer and then halved in subsequent layer transitions. The SELU activation function was applied to estimate the R/L parameter as it mitigates the vanishing gradient problem, which could lead to inappropriate weight and bias updates during the learning process. Several hyperparameters involved in the training process, such as the learning rate and training epoch, have been fine-tuned to find optimal values once the model achieves a testing accuracy of 95%. The learning rate is the increment utilized in the cost function optimization process, while the training epoch denotes the number of training iterations. The single-frequency DNN

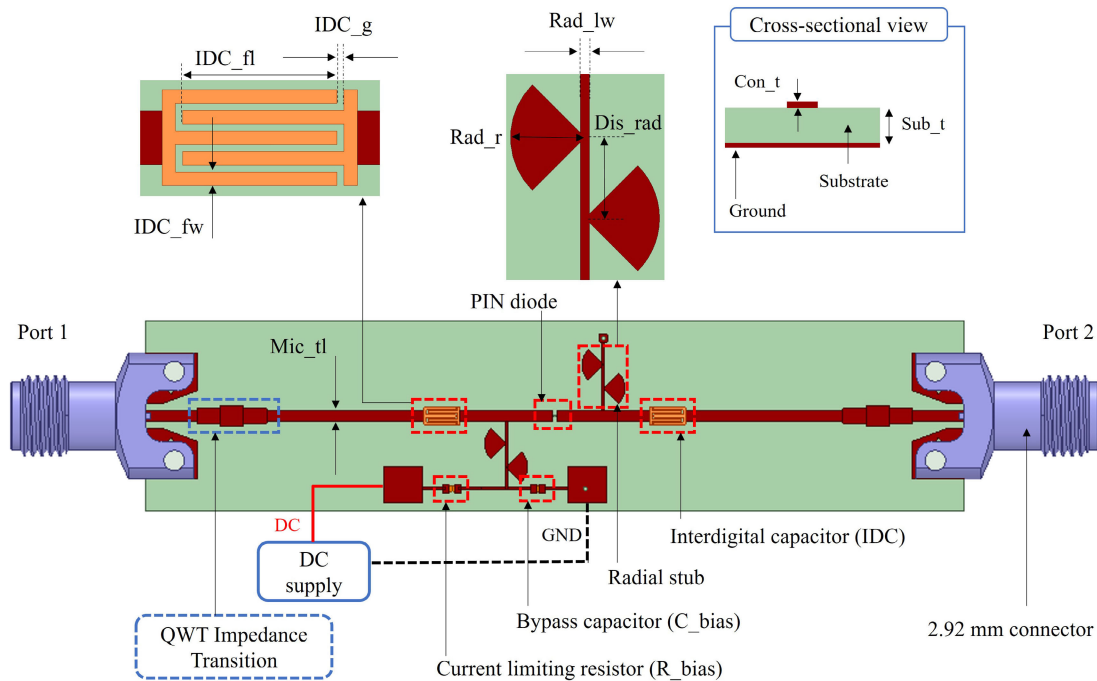


FIGURE 3. Proposed design of the microstrip measurement fixture, which the diameters are given in Table 1.

model was subsequently extended into a multi-frequency model demonstrated in Fig. 4(b), covering our frequency of interest spanning from 27 GHz to 30 GHz. In our method, an optimal DNN model is completed once achieving the above mentioned target training and testing accuracy. This involves optimizing several crucial parameters, including the number of hidden layers. It is worth noting that the number of hidden layers can severely increase the model complexity and training time consumption. After several trials on varying the number of hidden layers, we determined an optimal training performance with a 7-hidden layer model, which has been discussed comprehensively in our recently published works [26], [27].

It should be noted that the accuracy of the DNN model significantly relies on the input training dataset, which can increase the complexity of the model. Collecting plenty of data requires an extensive amount of time, and a reasonable range for the predefined parameters should be carefully considered. The simplified equivalent circuit in Fig. 1 considered both diode packaging effect and the parasitics due to soldering the diode on a PCB. From the measurement of a p-i-n diode, its transmission response S_{21} has been captured, calibrated, and processed for characterization which contains the characteristics of its package and soldering effects in addition to the diode. The simplified equivalent circuit of the p-i-n diode in its forward bias consists of a series connected resistance and inductance, and this circuit was modeled in HFSS by varying one parameter at a time to avoid possible failure due to excessive amount of simulations. The data collection for the R/L parameter was predefined

TABLE 2. Simulation data collection of forward-biased p-i-n diode for DNN model.

DNN Model	Configured "L"	Configured "R"
"R" Prediction	(Fixed), $L = 0.05$ nH	$0.25 \Omega - 20 \Omega$, increased by 0.25Ω
"L" Prediction	0.05 nH - 1.30 nH, increased by 0.05 nH	(Fixed), $R = 0.25 \Omega$

based on the component datasheet. For instance, a DNN model to predict the p-i-n diode resistance in our method comprises 80 simulations. These simulations are obtained by varying the resistance from 0.25Ω to 15Ω with 0.25Ω increments, and a fixed inductance of 0.05 nH. Table 2 presents the configuration of the two DNN models used to estimate the resistance and inductance of the p-i-n diode in its forward bias state. It is worth noting that these collected responses were later calibrated with the three TRL tx-line standards to accurately obtain the de-embedded response of the p-i-n diode before feeding it into the DNN model for training.

III. MEASUREMENT SETUP

The proposed design of the DUT measurement fixture and its corresponding tx-line standards for TRL calibration were fabricated. Fig. 5 depicts the entire measurement setup, where we connect the DUT test fixture to a network analyzer (Anritsu MS46122B) for capturing the S_{21} responses of the test sample. Simultaneously, a DC supply (ROHDE & SCHWARZ NGE100) is employed to bias the p-i-n diode

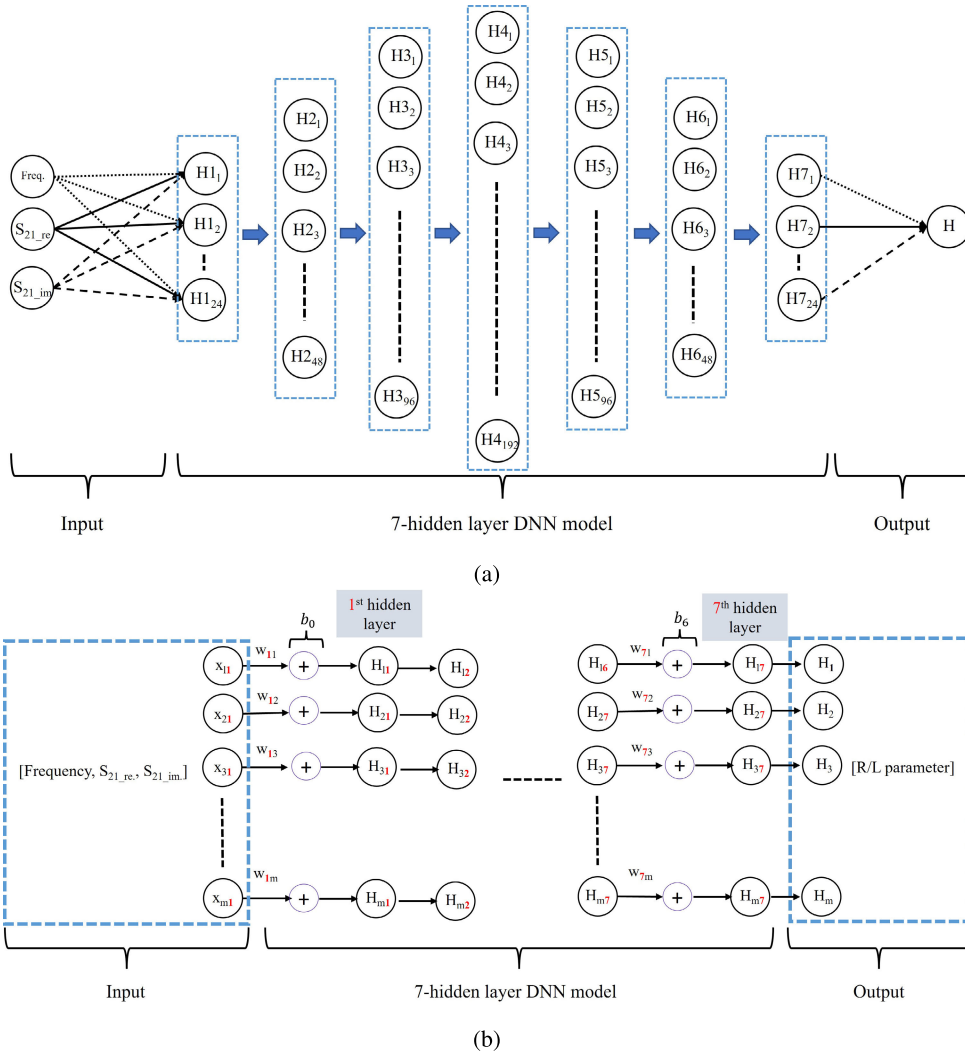


FIGURE 4. Schematic of the proposed 7-hidden layer DNN model: (a) Single-frequency, (b) Multi-Frequency.

at various biasing currents. A computer is used to set up the measurement configuration and view the responses of the measuring sample. Since we are interested in measuring the R-L electrical parameters of p-i-n diode in the 5G high-band, a frequency range from 27 GHz to 30 GHz has been designated for this measurement.

To mitigate the measurement uncertainties arising from instruments and other essential components involved in the measurement process, we performed a well-known short-open-load-through (SOLT) calibration using the VNA standard calibration kit. This calibration procedure effectively eliminates inaccuracies attributable to measurement equipment and redefines the reference plane of the measurement from the VNA connectors to the 2.92 mm connectors interface. However, an additional TRL calibration is applied in our method to extend the measurement plane beyond the connector and encompass the DUT section.

We measured the responses of the through, reflect, and line tx-line standard for the TRL calibration, respectively.

These specific measurements do not require a DC power supply, as there is no p-i-n diode integrated into the structure. For the measurement of the p-i-n diode, a DC power supply is connected to the bias TEE structure as illustrated in Fig. 3. We measured the diode in three DC biasing conditions, 1 mA, 5 mA, and 7 mA. From the measured responses of the DUT at each biasing current and TRL tx-line standards, we applied the calibration to obtain only the response of the p-i-n diode for each case. It is worth noting that there were no significant changes in the DUT responses for other biasing currents beyond 7 mA, based on the p-i-n diode model used in our measurement. Therefore, we selected the aforementioned three biasing conditions for the R-L electrical parameter retrieval of the p-i-n diode using the DNN-based extraction method in our research.

IV. RESULTS

The measurement data of the MA4AGP907 p-i-n diode was calibrated with a TRL calibration technique, and we obtained

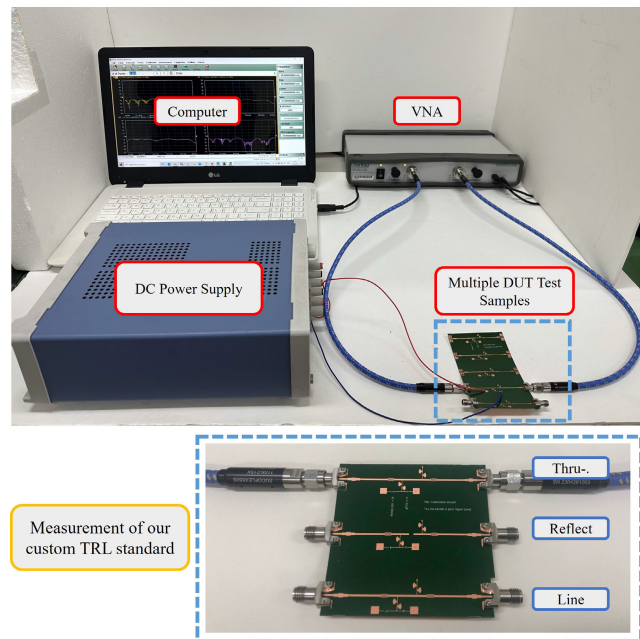


FIGURE 5. Measurement setup.

the response of the diode for 1 mA, 5 mA, and 7 mA accordingly. In Fig. 6(a), both the reflection coefficient (S_{11}) and the transmission coefficient (S_{21}) of the p-i-n diode are depicted at a DC biasing current of 7 mA. We noticed that the calibrated responses were improved significantly due to the removal of the effects from the measurement fixture. It should be noted that accurate calibration results are crucial for this DNN method since it exclusively relies on the training S_{21} complex data, which determines the transmissible power based on the electrical properties of the diode. Fig. 6(b) illustrates the calibrated responses for the three DC biasing conditions of the p-i-n diode. Notably, there is a discernible decrease in insertion loss as the biasing current is increased from 1 mA to 7 mA. The fluctuations across the frequency range of 27 GHz to 30 GHz can be attributed to the non-constant R-L electrical characteristics of the p-i-n diode within the observed frequency spectrum, and the specific configuration of the measurement environment.

We compared the measurement results from multiple test samples of the same p-i-n diode model, and obtained similar results that assure the reliability of our measurements. Furthermore, we provide a comparison between the S_{21} responses of the p-i-n diode in Fig. 7 between our calibrated data and the data provided by the manufacturer [28]. Our observations indicate that comparable results were attained for the observed DC biasing current of 5 mA in both datasets. However, our measurements tend to exhibit slightly higher losses, attributable to the design of integrated DC bias network in the test fixture and its corresponding TRL calibration standards. Hence, the calibrated results are applicable for subsequent processing with our DNN model, facilitating the estimation of the R-L electrical parameters of the p-i-n diode.

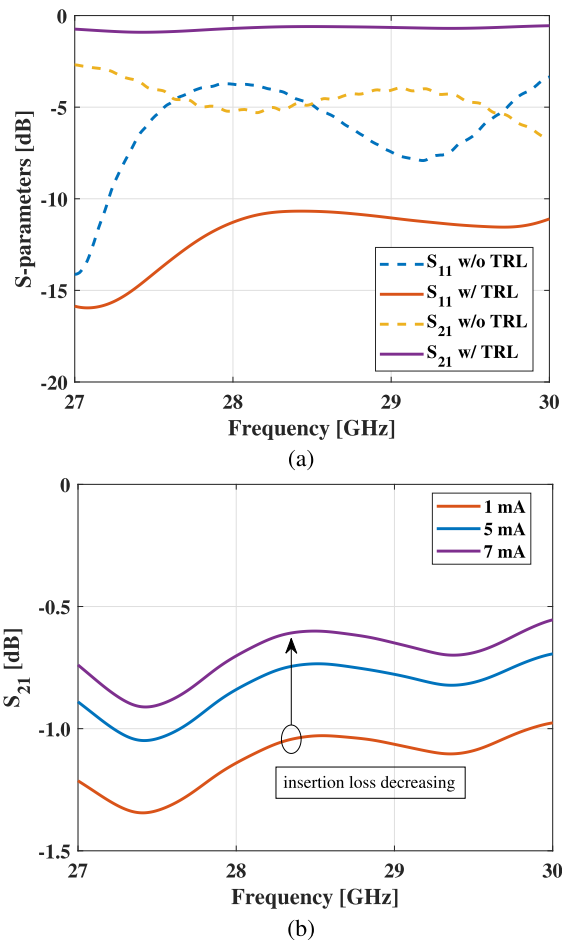


FIGURE 6. Measured S-parameters of the MA4GP907 p-i-n diode: (a) Responses without(w/o) and with(w/) TRL calibration (DC bias of 7 mA), (b) Calibrated responses of the diode at three DC biasing currents (1 mA, 5 mA, and 7 mA).

The complex S_{21} information corresponding to each DC biasing condition of the p-i-n diode has been input into our trained DNN model. The estimated resistance and inductance values are presented in sub-figures (a) and (b) of Fig. 8, respectively. It is worth noting that the extracted results (R/L) of a p-i-n diode are frequency-dependent. We determine its resistance and inductance from the extracted results of the DNN model for R and L prediction, respectively. Each DNN model was configured to have one parameter fixed while varying the other during training, e.g., fixed R while varying L. This is to investigate the frequency-dependent inductance with a minimal effect of the resistance and reduce the simulation time by having a smaller number of R-L permutations. Our method successfully retrieves R-L parameters within the frequency range of 27 GHz to 30 GHz, revealing gradual variations for all the applied DC bias conditions. The estimated resistance shows a consistent decrease as frequency increases, while it also decreases when the DC biasing current is raised from 1 mA to 7 mA. Given the substantial discrepancies losses in the S_{21} of the measurement data and the datasheet [28],

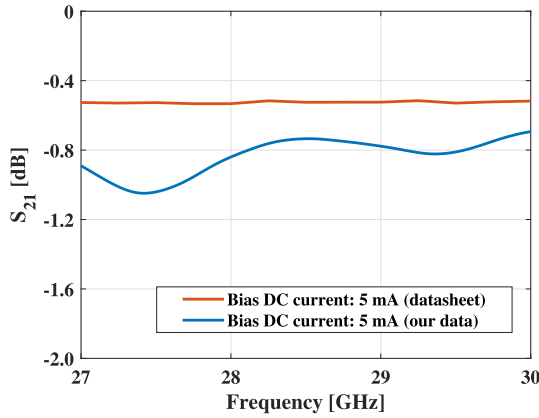


FIGURE 7. Comparison between the calibrated measurement data and datasheet of the MA4AGP907 p-i-n diode.

we expect that the diode will provide higher resistance values in the actual PCB implementation with DC biasing network. As a result, we obtained the resistance of 11Ω at 28 GHz for the DC bias of 5 mA which is bigger than the datasheet that affirms the correctness of our estimated results. In contrast to resistance, the inductance tends to increase with ascending frequency until around 28.5 GHz based on the prediction. A subtle difference in the estimated results was observed for each case in the frequency of interest. It is worth emphasizing that our method can provide the R-L parameters extraction in a frequency-dependent manner, significantly enhancing the accuracy of p-i-n diode characteristic modeling in simulations.

We offer a comparison between our proposed DNN-based extraction method of the electrical parameters of p-i-n diode and the relevant existing techniques, as detailed in Table 3, to underscore the contribution and novelty of our approach. It presents an alternative means of extracting the electrical parameters of the diode within the 5G high band, specifically spanning the frequency range from 27 GHz to 30 GHz. The DNN-based extraction approach exclusively relies on S_{21} information from the measured diode response. Moreover, our method demonstrates the potential for extracting frequency-dependent characteristics over a given range with moderate results by using full-wave 3D electromagnetic simulation software. This simulation incorporates a DC biasing network, enhancing the ability of the method to yield emulated diode characteristics. Notably, our approach exhibits proficiency in obtaining diode properties with a reduced data input from measurements, a trait particularly advantageous in contrast to analytical solutions. Analytical methods often necessitate more information on the measurement and assumptions for their calculations, which can significantly impair the accuracy of the extracted p-i-n diode electrical parameters. Our proposed method requires less input data for p-i-n diode characterization, which is a useful parameters for designing reconfigurable antennas within the 5G high band.

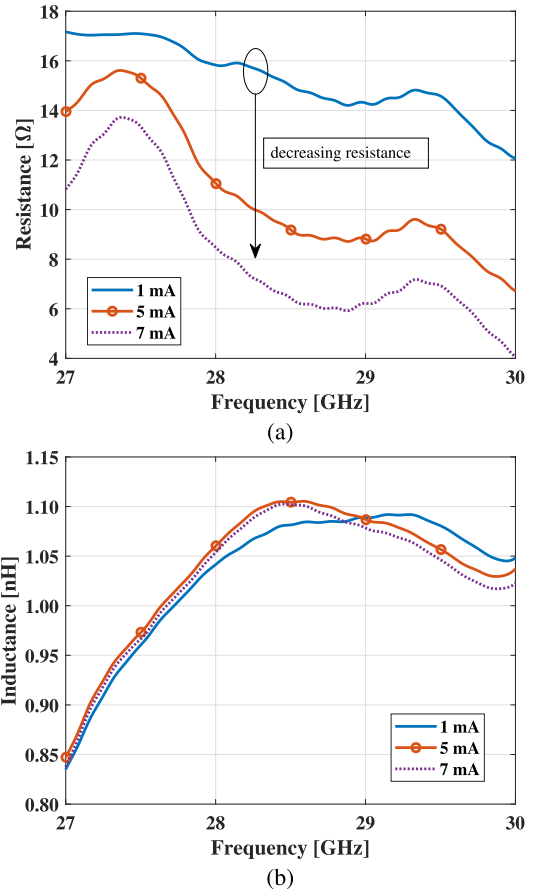


FIGURE 8. Predicted resistance and inductance of MA4AGP907 p-i-n diode: (a) Resistance [Ω], (b) Inductance [nH].

V. CONCLUSION

This paper presented an alternative approach for extracting the electrical parameters of a p-i-n diode in its forward bias state using a DNN-based method, covering the frequency range from 27 GHz to 30 GHz. The approach involves training the proposed 7-hidden-layer DNN model which has been trained with simulated S_{21} data obtained from HFSS. After achieving a defined optimal model with a training accuracy of 95%, we applied this model to estimate the R-L parameters of p-i-n diode from the calibrated S_{21} responses. Our proposed method is capable of providing a frequency-dependent parameter extraction using solely S_{21} information. This alternative and novel approach reduces errors in the extracted parameters incurred with analytical or curve-fitting methods. We validated our approach by extracting the electrical parameters of the MA4AGP907 p-i-n diode at Ka-band and obtained reasonable results. The extracted resistance decreases as we increase the biasing current from 1 mA to 7 mA, and also decreases as the frequency increases. Meanwhile, the estimated inductance exhibits an increasing trend with frequency, as indicated in our findings. This information will be beneficial for researchers, working on designing reconfigurable antennas at the 5G high band using the aforementioned p-i-n diode model to optimize the

TABLE 3. Comparison between the proposed DNN-based and other relevant methods of the electrical parameter extraction of p-i-n diode.

Method	Feature	Frequency [GHz]	Accuracy	Computational Cost
Curve fitting [15]	<ul style="list-style-type: none"> • BA682 diode [From Philips] • Apply separate bias TEE attached to the measurement fixture (vulnerable to measurement uncertainty) • Frequency independent extraction • Extracted parameter: Resistance (forward bias) 	L-band (1.30 – 1.50)	Roughly approximated extraction with curve fitting method	Less complexity and computational cost
Analytical extraction using ABCD matrix [16]	<ul style="list-style-type: none"> • HSMS 282B diode [From Broadcom] • Frequency-dependent extraction from only S-parameters (S_{11}, S_{12}, S_{21}, S_{22}) • Extracted parameters: resistance; capacitance (forward bias) 	X-band (0.1 – 10)	Extracted results are vulnerable to measurement errors	Less complexity and computational cost
DNN-based extraction [This work]	<ul style="list-style-type: none"> • MA4AGP907 p-i-n diode [From Macom] • Frequency-dependent extraction from only S-parameters (S_{21}) • Integrated design of bias TEE with radial stub and IDC into the fixture • Extracted parameters: resistance; inductance (forward bias) 	Ka-band (5G High band, 27 – 30)	Moderate results due to simplified equivalent circuit of the modeling p-i-n diode	More complexity and high computational cost (resource and time) due to collection of data for training DNN model Model complexity increase with more extracting parameters

design based on the provided R-L electrical characteristics of a p-i-n diode. The diode used for antenna design involves only a small-signal input, hence the non-linear effects due to high frequency were not considered in this research. Additional investigation for this non-linear analysis of the diode can be taken into consideration in future work.

ACKNOWLEDGMENT

The authors thank Sebastian Verho for providing helpful review and insight to improve their paper.

REFERENCES

- [1] Z. Wang, S. Liu, and Y. Dong, "Compact wideband pattern reconfigurable antennas inspired by end-fire structure for 5G vehicular communication," *IEEE Trans. Veh. Technol.*, vol. 71, no. 5, pp. 4655–4664, May 2022, doi: 10.1109/TVT.2022.3152354.
- [2] C. G. Christodoulou, Y. Tawk, S. A. Lane, and S. R. Erwin, "Reconfigurable antennas for wireless and space applications," *Proc. IEEE*, vol. 100, no. 7, pp. 2250–2261, Jul. 2012, doi: 10.1109/JPROC.2012.2188249.
- [3] B. Rana, I. G. Lee, and I. P. Hong, "Experimental characterization of 22 electronically reconfigurable 1 bit unit cells for a beamforming transmitarray at X band," *J. Electromagn. Eng. Sci.*, vol. 21, no. 2, p. 153–160, 2021.
- [4] J. Costantine, Y. Tawk, S. E. Barbin, and C. G. Christodoulou, "Reconfigurable antennas: Design and applications," *Proc. IEEE*, vol. 103, no. 3, pp. 424–437, Mar. 2015, doi: 10.1109/JPROC.2015.2396000.
- [5] N. O. Parchin, H. J. Basherlou, Y. I. A. Al-Yasir, A. M. Abdulkhaleq, and R. A. Abd-Alhameed, "Reconfigurable antennas: Switching techniques—A survey," *Electronics*, vol. 9, no. 2, p. 336, Feb. 2020.
- [6] S. N. M. Zainarry, N. Nguyen-Trong, and C. Fumeaux, "A frequency- and pattern-reconfigurable two-element array antenna," *IEEE Antennas Wireless Propag. Lett.*, vol. 17, no. 4, pp. 617–620, Apr. 2018, doi: 10.1109/LAWP.2018.2806355.
- [7] A. Grau Besoli and F. De Flaviis, "A multifunctional reconfigurable pixelated antenna using MEMS technology on printed circuit board," *IEEE Trans. Antennas Propag.*, vol. 59, no. 12, pp. 4413–4424, Dec. 2011, doi: 10.1109/TAP.2011.2165470.
- [8] M. N. M. Kehn, Ó. Quevedo-Teruel, and E. Rajo-Iglesias, "Reconfigurable loaded planar inverted-F antenna using varactor diodes," *IEEE Antennas Wireless Propag. Lett.*, vol. 10, pp. 466–468, 2011, doi: 10.1109/LAWP.2011.2153174.
- [9] C. Deng, D. Liu, B. Yektakhah, and K. Sarabandi, "Series-fed beam-steerable millimeter-wave antenna design with wide spatial coverage for 5G mobile terminals," *IEEE Trans. Antennas Propag.*, vol. 68, no. 5, pp. 3366–3376, May 2020, doi: 10.1109/TAP.2019.2963583.
- [10] S. Verho, V. T. Nguyen, and J.-Y. Chung, "A 4×4 active antenna array with adjustable beam steering," *Sensors*, vol. 23, no. 3, p. 1324, Jan. 2023, doi: 10.3390/s23031324.
- [11] W. E. Doherty and R. D. Joos, "The PIN diode circuit designershandbook," *Microsemi Corp.*, vol. 1, pp. 1–137, 1998.
- [12] G. Jin, C. Deng, J. Yang, Y. Xu, and S. Liao, "A new differentially-fed frequency reconfigurable antenna for WLAN and sub-6GHz 5G applications," *IEEE Access*, vol. 7, pp. 56539–56546, 2019, doi: 10.1109/ACCESS.2019.2901760.
- [13] H. Dildar, F. Althobiani, I. Ahmad, W. U. R. Khan, S. Ullah, N. Mufti, S. Ullah, F. Muhammad, M. Irfan, and A. Glowacz, "Design and experimental analysis of multiband frequency reconfigurable antenna for 5G and sub-6 GHz wireless communication," *Micromachines*, vol. 12, no. 1, p. 32, Dec. 2020.
- [14] M. Patriotis, F. N. Ayoub, Y. Tawk, J. Costantine, and C. G. Christodoulou, "A millimeter-wave frequency reconfigurable circularly polarized antenna array," *IEEE Open J. Antennas Propag.*, vol. 2, pp. 759–766, 2021, doi: 10.1109/OJAP.2021.3090908.
- [15] K. T. Trinh, J. Feng, S. H. Shehab, and N. C. Karmakar, "1.4 GHz low-cost PIN diode phase shifter for L-band radiometer antenna," *IEEE Access*, vol. 7, pp. 95274–95284, 2019, doi: 10.1109/access.2019.2926140.
- [16] A. Allothman, "Analytical extraction method of a large-signal diode equivalent circuit model using the ABCD matrix," *TechRxiv*, 2022, doi: 10.36227/techrxiv.21350754.v1.
- [17] A. Zhang and J. Gao, "Comprehensive analysis of linear and non-linear equivalent circuit model for GaAs-PIN diode," *IEEE Trans. Ind. Electron.*, vol. 69, no. 11, pp. 11541–11548, Nov. 2022, doi: 10.1109/TIE.2021.3125563.
- [18] T. Liu, L. Xu, Y. He, H. Wu, Y. Yang, N. Wu, X. Yang, X. Shi, and F. Wei, "A novel simulation method for analyzing diode electrical characteristics based on neural networks," *Electronics*, vol. 10, no. 19, p. 2337, Sep. 2021, doi: 10.3390/electronics10192337.
- [19] J.-S. Kang, "Free-space unknown thru measurement using planar offset short for material characterization," *J. Electromagn. Eng. Sci.*, vol. 22, no. 5, pp. 555–562, Sep. 2022.

- [20] R. S. Beerasha, A. M. Khan, and H. V. Manjunath-Reddy, "Design and optimization of interdigital capacitor," in *Int. J. Res. Eng. Technol.*, vol. 5, no. 33, pp. 73–78, Nov. 2016.
- [21] N. Jana, M. K. Mandal, and R. Shaw, "An improved design of a bias tee using a modified radial stub," in *IEEE MTT-S Int. Microw. Symp. Dig.*, Dec. 2019, pp. 1–4, doi: [10.1109/IMaRC45935.2019.9118616](https://doi.org/10.1109/IMaRC45935.2019.9118616).
- [22] Q.-J. Zhang, K. C. Gupta, and V. K. Devabhaktuni, "Artificial neural networks for RF and microwave design—from theory to practice," *IEEE Trans. Microw. Theory Techn.*, vol. 51, no. 4, pp. 1339–1350, Apr. 2003, doi: [10.1109/TMTT.2003.809179](https://doi.org/10.1109/TMTT.2003.809179).
- [23] K. V. Babu, S. Das, G. N. J. Sree, S. K. Patel, M. P. Saradhi, and M. R. N. Tagore, "Design and development of miniaturized MIMO antenna using parasitic elements and machine learning (ML) technique for lower sub 6 GHz 5G applications," *AEU Int. J. Electron. Commun.*, vol. 153, Aug. 2022, Art. no. 154281.
- [24] M. Elkattan and A. H. Kamel, "Estimation of electromagnetic properties for 2D inhomogeneous media using neural networks," *J. Electromagn. Eng. Sci.*, vol. 22, no. 2, pp. 152–161, Mar. 2022.
- [25] M. Lavanya and R. Parameswari, "A multiple linear regressions model for crop prediction with Adam optimizer and neural network Miraonn," *Int. J. Adv. Comput. Sci. Appl.*, vol. 11, no. 4, pp. 1–6, 2020.
- [26] L. Nov, J.-Y. Chung, and J. Park, "Broadband permittivity characterization of a substrate material using deep neural network trained with full-wave simulations," *IEEE Access*, vol. 10, pp. 48464–48471, 2022, doi: [10.1109/ACCESS.2022.3172300](https://doi.org/10.1109/ACCESS.2022.3172300).
- [27] T. Chrek, L. Nov, and J. Chung, "Deep neural network for retrieving material's permittivity from S-parameters," *Microw. Opt. Technol. Lett.*, vol. 65, no. 2, pp. 418–424, Feb. 2023.
- [28] *MA4AGP907*. Accessed: Jan. 22, 2023. [Online]. Available: www.macom.com/products/product-detail/MA4AGP907



LIHOUR NOV (Student Member, IEEE) was born in Cambodia, in 1997. He received the M.S. degree in integrated IT engineering from the Seoul National University of Science and Technology, South Korea, in 2020, where he is currently pursuing the Ph.D. degree in integrated IT engineering. He is a Research Assistant with the Electromagnetic Measurement and Application (EMMA) Laboratory, Seoul National University of Science and Technology. His current research interest includes material characterization.



THORN CHREK received the B.Sc. degree in telecommunication and electronic engineering from the Royal University of Phnom Penh, Cambodia, in 2019, and the M.S. degree in electrical and information engineering from the Seoul National University of Science and Technology, South Korea, in 2023, where he is currently pursuing the Ph.D. degree in electrical and information engineering. His research interests include the field of transmission line design, deep learning deployed to material characterization, and antenna design.



JAE-YOUNG CHUNG (Senior Member, IEEE) received the B.S. degree in electrical engineering from Yonsei University, Seoul, South Korea, in 2002, and the M.S. and Ph.D. degrees in electrical engineering from The Ohio State University, Columbus, OH, USA, in 2007 and 2010, respectively. From 2002 to 2004, he was an RF Engineer with Motorola, South Korea. From 2010 to 2012, he was an Antenna Engineer with Samsung Electronics. He is currently an Associate Professor with the Department of Electrical and Information Engineering, Seoul National University of Science and Technology. His research interests include electromagnetic measurement and antenna design.

• • •